Materials Science in Semiconductor Processing 42 (2016) 204–209

Contents lists available at ScienceDirect

Materials Science in Semiconductor Processing

journal homepage: www.elsevier.com/locate/mssp

RF plasma treatment of shallow ion-implanted layers of germanium

P.N. Okholin [a], V.I. Glotov [b], A.N. Nazarov [a,*], V.O. Yuchymchuk [a], V.P. Kladko [a], S.B. Kryvyi [a], P.M. Lytvyn [a], S.I. Tiagulskyi [a], V.S. Lysenko [a], M. Shayesteh [c], R. Duffy [c]

[a] V. Lashkaryov Institute of Semiconductor Physics, NASU, Prospekt Nauky 41, Kyiv 03028, Ukraine
[b] Institute of Microdevices, NASU, Kyiv 04136, Ukraine
[c] Tyndall National Institute, University College Cork, Lee Maltings, Prospect Row, Cork, Ireland

ARTICLE INFO

Article history:
Received 27 May 2015
Received in revised form
11 August 2015
Accepted 17 August 2015
Available online 28 August 2015

Keywords:
Implanted germanium
Plasma annealing
Rapid thermal annealing
Raman spectroscopy
X-ray diffraction

ABSTRACT

RF plasma annealing (RFPA) and rapid thermal annealing (RTA) of high-dose implanted n-type and p-type amorphized Ge layers have been studied by Raman scattering spectroscopy and X-ray diffraction techniques. It is shown that recrystallization of n-Ge implanted by BF_2^+ ions requires higher RTA temperatures and power density of RFPA as compared to p-Ge implanted by P^+ ions with the same dose. The RFPA has been performed at considerably lower temperatures than RTA and resulted in the formation of a sharp interface between the implanted and underlying Ge layers both for BF_2^+ ion implantation and P^+ ions implantation.

1. Introduction

Shallow drain/source p–n junction formation is a key requirement in production of advanced Si and Ge devices. Germanium has considerable advantages in comparison with silicon due to high electron/hole mobility and low temperature activation of implanted impurities [1]. However, diffusion coefficients for donor impurities in germanium, e.g., for phosphorus, are rather high [1], which hampers the formation of super-shallow n^+/p junctions. Therefore in the case of Ge-based devices one should avoid the high-temperature annealings that are traditionally used to eliminate the implantation-induced defects and to activate of implanted impurity [2]. At present, the most widely used methods for annealing of shallow implanted layer in Ge are: low-temperature annealing, such as solid-phase-epitaxial-regrowth (SPER) [3] and microwave annealing (MA) [4]; short time annealing, such as rapid thermal annealing (RTA) [5], flash-lamp annealing (FLA) [6] or laser annealing (LA) [7]. As an alternative the low-temperature RF plasma annealing (RFPA) can be used; this method was employed successfully for the annealing of thin implanted Si layers [8] but up to now it was not applied to implanted Ge layers. It should be noted that in the case of high-dose ion implantated Si layers, when the amorphous subsurface layer is formed, low-temperature RF plasma annealing does not lead to the recrystallization of the amorphous Si subsurface layer but creates the completely mechanically relaxed amorphous layer [9]. Due to considerably lower recrystallization temperature of amorphous Ge layers as compared to amorphous Si layers [1], and to the fact that RF plasma treatment anneals the defects within a thin surface layer [10], it should be expected that the RFPA could be successfully applied to crystallize shallow amorphous Ge layer and to form shallow p–n junctions. The present paper considers the first fundamental stage of the study of a low-temperature RF plasma treatment associated with a structural transformation of thin amorphous implanted Ge layers and compares with more frequently used method of annealing-RTA.

2. Experimental

The monocrystalline germanium (Ge) wafers with $<100>$ orientation were fabricated by liquid encapsulated Czochralski (LEC) method and were polished on the front side. The Ge wafers were mechanically relaxed that was confirmed by Raman scattering (RS) spectroscopy measurements (see Fig. 1(b)). The n-type Ge wafer with carriers concentration about 10^{14} cm^{-3} was implanted by BF_2^+ ions with the energy of 20 keV and the dose of 1×10^{15} ions/cm^2. The p-type Ge wafer with carriers concentration about $(7\pm2)\times10^{16}$ cm^{-3} was implanted by P^+ ions with the energy 12 keV and the same dose of implantation. Energies of the ions were chosen to obtain equal projected lengths for different implanted ions. In both cases the maximum of ion distribution

* Corresponding author.
E-mail address: nazarov@lab15.kiev.ua (A.N. Nazarov).

http://dx.doi.org/10.1016/j.mssp.2015.08.028

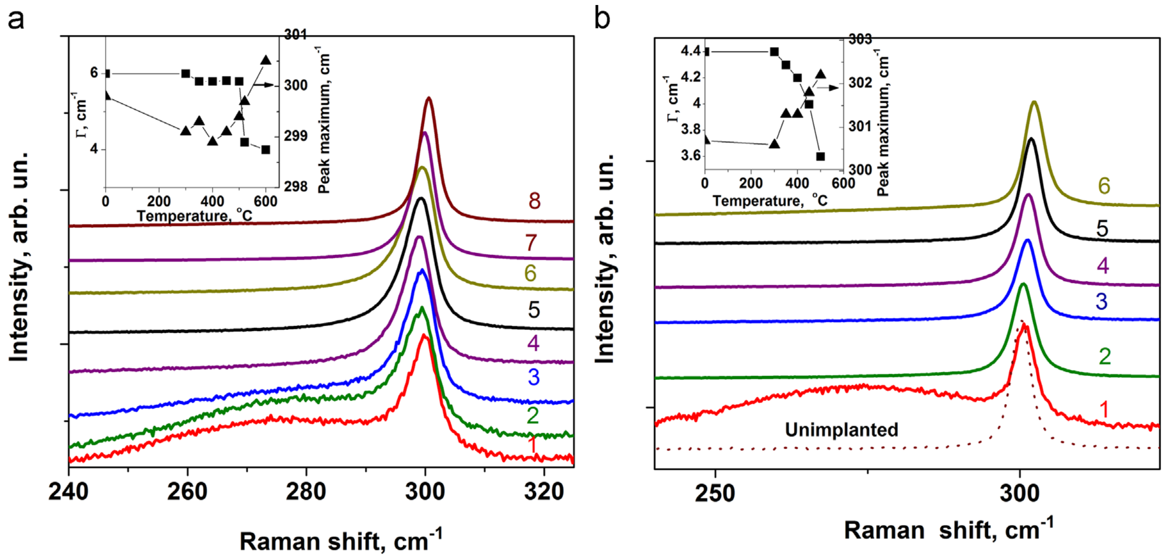

Fig. 1. Normalized RS spectra for n-Ge implanted by BF_2^+ ions (a) and p-Ge implanted by P^+ ions (b). The treatment parameters: 1. As-implanted samples (before RTA); 2. $T=300$ °C; 3. 350 °C; 4. 400 °C; 5. 450 °C; 6. 500 °C; 7. 520 °C; 8. 600 °C ($t=15$ s). The insets in figures (a) and (b) show both the half-width, Γ, (■) and the maximum position (▲) of the "crystalline" peak as a function of RTA temperature.

profile was situated about 15 nm from Ge surface. The profiles simulation was performed by SRIM code.

The implanted Ge layer was annealed by RTA methods in nitrogen ambient in temperature range from 300 to 550 °C during 15 s. The RF plasma treatment (13.56 MHz) was performed in diode type reactor in the forming gas (90% N_2+10% H_2) atmosphere [8]. The samples were located on the heated (up to 200 °C) RF electrode. The RF plasma power density was varied from 0.5 to 2.0 W/cm^2, the treatment duration was 10 min. The sample temperature for plasma treatment was monitored in situ using special calibrated thermal paints that were deposited on the back side of the samples. Calibration of the thermal paint has been done in a standard oven. Results of the measurements are shown in Fig. 5 (c) in the paper [11].

The phase composition of the samples was studied by Raman scattering (RS) spectroscopy at room temperature. The RS spectra were studied using double monochromator DFS-52 equipped with Andor CCD camera. YAG laser ($\lambda=532$ nm, $P<10$ mW) was used for excitation. Information on the deformations distribution near the Ge surface was obtained by the X-ray diffraction (XRD) measurements in the $\omega-2\theta$ regime using CuKα1 line (Philips X'Pert-MRD diffractometer was employed). The samples were scanned in the vicinity of (004) Bragg's reflex with a step of 0.001°. Surface morphology was studied by atomic force microscopy (AFM) using NanoScope IIIa Dimension 3000.

3. Results and discussion

3.1. Raman scattering spectra

The RS spectra of implanted and RTA treated n-Ge and p-Ge samples are presented in Fig. 1(a) and (b), respectively. The spectrum 1 corresponds to the implanted Ge samples and consists of the wide peak with the maximum at 273 cm^{-1} related to the amorphous Ge phase and the narrow asymmetric peak at 300 cm^{-1} which is ascribed to the crystalline Ge phase. In our case when the amorphous Ge layer has a thickness of about 20 nm (according to the SRIM simulation), and the penetration depth for the light with the wavelength of 532 nm is about 25 nm, the crystalline component from the Ge substrate is always present in the Raman spectrum. Asymmetry of the peak can be caused by additional light scattering by Ge nanocrystals [12] and stretched Ge layer [13].

After RTA of the implanted n-Ge at temperatures from 300 to 350 °C the intensity of the wide peak, that corresponds to the amorphous phase, decreases; this peak completely disappears in the spectra of the samples annealed at 400 °C and higher (Fig. 1 (a)). It should be noted that the "crystalline" peak in RS spectrum for the RTA at 400 °C has considerably larger half-width (~ 6.5 cm^{-1}) than in the case of initial unimplanted sample (3.3 cm^{-1}) and the maximum is somewhat shifted to lower frequencies (see the inset in Fig. 1(a)). These features can be associated with appearance of Ge nanocrystals in the annealed implanted layer, which results in a low-frequency shift of the Ge crystalline peak [12] and to effect on his broadening.

The smaller the size of Ge nanocrystallites results in more red shift of the Ge "crystalline" peak. When the temperature of RTA is higher than 400 °C the size of nanocrystallites in the implanted layer increases, and after the RTA at 600 °C the implanted layer is totally transformed into monocrystalline Ge layer. The effect of the increase of nanocrystallites size leads to the blue shift of Ge "crystalline" peak, and after the RTA at 600 °C the half-width and position of the crystalline peak is almost the same as in the case of the initial unimplanted n-Ge. However, the effect of tensile stresses in the implanted Ge layer on the RS "crystalline" peak cannot be neglected. It is known, that tensile stress in implanted semiconductor layers varies along the depth of the layer [14] that can cause the "crystalline" peak broadening and red shifting. Relaxation of the tensile stresses during the annealing has to restore the peak position and half-width. In our case we, probably, observe the influence of both factors.

Furthermore, the observed value of crystallization temperature (about 400 °C) is considerably higher than the one obtained for the phosphorus-implantated Ge (see Fig. 1(b)). This observation can be attributed to two effects: firstly, implantation with more heavy ions (BF_2^+ regarding to P^+) results in more amorphized (more damaged) layer; secondly, introduction of fluorine into the damaged germanium (dose about 2×10^{15} cm^{-2}) leads to stabilizing of defects and, thus, can also increase the temperature of amorphous layer recrystalization. Moreover, it is known [15] that at the annealing temperature about 500 °C fluorine can passivate vacancies in Ge and form the F_nV_m cluster; this process leads to the relaxation of the tensile stresses and enhanced boron diffusion in the implanted material [16]. Probably, the observed effect of sharp decrease of "crystalline" peak half-width (see the inset in Fig. 1(a)) can be related to the process of vacancy passivation by fluorine.

The RTA of p-Ge implanted by P^+ ions significantly differs from the RTA of n-Ge implanted by $BF_2{}^+$ ions. The RTA at 300 °C results in the complete crystallization of the amorphous phase in the Ge thin layer (Fig. 1(b)). Besides, the half-width of the peak at 300 cm^{-1} is relatively small (Γ=4.4 cm^{-1}) even after the ion implantation, that is an evidence of absence of big stresses and formation of small nanocrystallites. At increasing temperature of the RTA process the high-frequency shift and gradual reduction of the half-width of the "crystalline" peak have been observed (inset in Fig. 1(b)). The observed RS peak shift can be caused by the compressive stresses which are usually observed in the end-of-range (EOR) defect region saturated with interstitial atoms and located deeper than the amorphous implanted layer. Thus, the annealing of the thin amorphous implanted layer which has tensile stresses and effect of compressive stress in the substrate has to results in high-frequency shift of the "crystalline" RS peak.

The RF plasma treatment of the implanted n-Ge leads to the annealing of amorphous phase in thin implanted layer at 200 °C with power density 1.75 W/cm^2 (Fig. 2(a)); note, that during this treatment the sample can be heated up to 320 °C [11]. The half-width of the "crystalline" peak in the RS spectrum is about 6 cm^{-1} that can be ascribed to different mechanical stresses in the surface (and in the bulk) of Ge layers as well as to the formation of Ge nanocrystallites in subsurface layer. Thus RF plasma treatment of BF_2^+-implanted thin Ge layer transforms amorphous layer into crystalline (or microcrystalline) one at lower temperature than RTA process, however, the concentration of defects in the layer remains still rather high.

RF plasma treatment of the P^+-implanted p-Ge leads to crystallization of the implanted surface layer at considerably lower temperature and power than in the case of the P^+-implanted n-Ge. At 100 °C and power density 0.9 W/cm^2 the thin implanted amorphous layer is completely recrystallized (spectrum 2, Fig. 2(b)). The temperature of the samples during such RF plasma treatment is about 200 °C [11]. RF power density rise (note that the sample was additionally heated up to 200 °C) resulted in the reduction of the "crystalline" peak half-width that is related to the decrease of defect concentration in the implanted layer. Because RF plasma treatment affects strongly only the thin surface layer of the semiconductor [8] it is natural to assume the reduction of tensile stresses (annealing of thin surface layer) in the samples with the increase of RF plasma power, that leads to high-frequency shift of the "cristalline" RS peak. A shift of the RS peak in range up to 303 cm^{-1} can be caused by compressive stresses of EOR defect region located deeper than the implanted layer.

3.2. X-ray diffraction

Fig. 3 presents XR diffractograms for implanted n-Ge and p-Ge. Diffractogram of initial implanted n-Ge (curve 1, Fig. 3(a)) shows a sloping shoulder on the left from zero, that corresponds to tensile stresses, and broad peak on the right from zero, is indicative of compressive stresses. Thus, during implantation of n-Ge by BF_2^+ ions the implantation defects are observed which stretch and compress of the crystalline layers of the Ge. Behavior of the left shoulder is related to strong surface layer amorphization, and the diffuse diffraction component (defects) of the XRD provides the main contribution to the form of diffraction reflection curve (DRC). RF plasma treatment at T=200 °C and P=0.75 W/cm^2 did not lead to considerable decrease of amorphous left shoulder (curve 2 in Fig. 3(a)) while the broad peak on the right from zero increased slightly that, probably, points to the increase of compression stresses in the EOR defect region. After the RF plasma treatment at T=200 °C and P=1.50 W/cm^2 we observe DRC with well expressed broad peak on the left from zero (curve 3, Fig. 3(a)) that attests a good quality crystallization of the thin surface layer of implanted n-Ge, which has tensile stresses, and presence of sharp interface between implanted and underlying layer. The RTA at 450 °C of the BF_2^+- implanted n-Ge results in crystallization of the surface amorphous layer that appears in DRC as a wide peak on the left side from the Bragg angle (curve 4 in Fig. 3(a)). This wide peak can correspond to a strongly deformed Ge layer with larger lattice constant in comparison with the bulk one. The observed broad peak is wider than the one observed in case of RF plasma treatment at T=200 °C and P=1.50 W/cm^2 that can indicate on wider tensile stress distribution in case of RTA. Because of a tensile stress distribution in ion implanted Ge layer is associated with distribution of the implanted impurity [14], it can mean that in case of RFPA the impurity distribution is sharper than after RTA.

DRC of the P^+-implanted p-Ge (curve 1 Fig. 3(b)) is considerably different than one for the as-implanted n-Ge (curve 1 Fig. 3(a)). In case of P^+-implanted p-Ge lightly expressed shoulders both on the left from zero and on the right from zero are

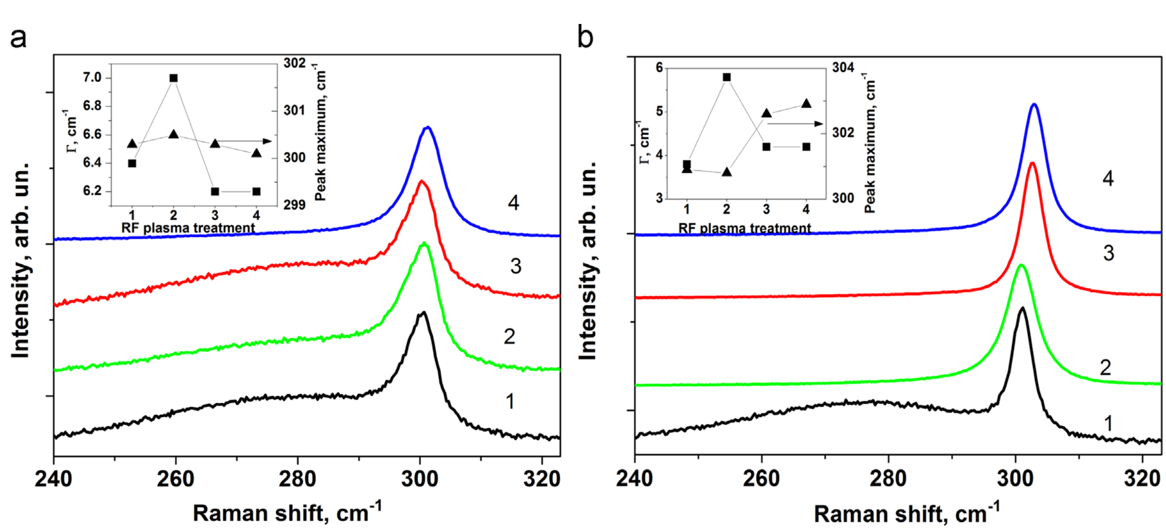

Fig. 2. Normalized RS spectra of n-Ge implanted by $BF_2{}^+$ ions (a) and p-Ge implanted by P^+ ions (b). The parameters of post-implantation RFPA trtment: 1. T=100 °C, P=0.55 W/cm^2; 2. T=100 °C, P=0.90 W/cm^2; 3. T=200 °C, P=0.75 W/cm^2; 4. T=200 °C, P=1.75 W/cm^2 (t=10 min). The insets in figures (a) and (b) show both the half-width, Γ, (■) and the maximum position (▲) of the "crystalline" peak as a function of RF plasma regime.

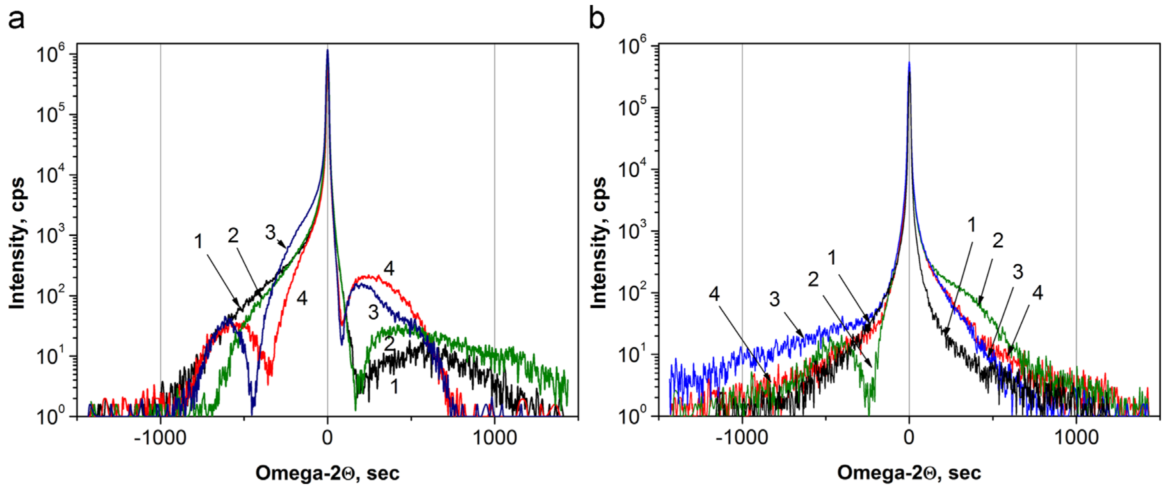

Fig. 3. The $\omega-2\theta$ diffractograms for BF_2^+-implanted n-Ge (a) and for P^+implanted p-Ge (b). The parameters of post-implantation treatments: 1. As-implanted sample; 2. RFPA, $T=200$ °C, $P=0.75$ W/cm^2 ($t=10$ min); 3. RFPA, $T=200$ °C, $P=1.50$ W/cm^2 ($t=10$ min); 4. RTA, $T=450$ °C, ($t=15$ s).

observed, that are related to small and distributed tensile and compress stresses in the p-Ge implanted layer, correspondingly. Therefore both RTA and RFPA of the P^+-implanted p-Ge result mainly in different stress distributions in comparison with n-Ge implanted samples (see Fig. 3(b)). So, for the RF plasma treatment at $T=200$ °C and $P=0.75$ W/cm^2 (curve 2, Fig. 3(b)), which recrystallizes thin amorphous layer (see Fig. 2(b)), good quality surface crystalline layer with a sharp interface between implanted and un-implanted Ge layers can be formed that is in the agreement with the results obtained by RS spectroscopy (curve 3, Fig. 2(b)). However a further increase of RFPA power resulted in a formation of strongly smoothed shoulder in the left side of the DRC (curve 3, Fig. 3(b)) that can be ascribed to tensile stresses strongly distributed in depth of Ge wafer.

After the RTA at 450 °C of the P^+-implanted p-Ge we observe a smooth DRC to the left of main peak and very similar curve in the right part of the peak (curve 4, Fig. 3(b)) that corresponds to fluent tensile and compress stress distributions in material. The DRC is a lightly assymetrical in side of the right part of the main peak that related to increased compress stresses in the material.

3.3. Effect of nonthermal factors at RF plasma treatment

To distinguish nonthermal factors which can lead to a reduction of the crystallization temperature of the implanted Ge samples, the control experiments with treatment of the samples by RF plasma discharge from the implanted side and the back side in the same technological process were carried out [17]. Fig. 4(a) demonstrates that RF treatment of the implanted side results in enhanced crystallization of amorphous implanted layer (disappearance of wide RS peak at 273 cm^{-1}), and a decrease of sloping shoulder in left side of the XRD curve (Fig. 4(b)), and the formation of sharp layer between implanted and underlying layers. RF plasma treatment of the back un-implanted side of the samples shows very small effect on thin amorphous layer (Fig. 4(a)) and changing of mechanical stresses (Fig. 4(b)), both tensile (on the left side from zero) and compression ones (on the right side from zero).

During RF plasma treatment the front side of the implanted samples can be affected by the following factors: temperature; UV and soft X-ray irradiation, alternating electric field, proton injection from plasma; low-energy electron and ion bombardment [8,18]. Under RF plasma treatment from back side of the sample,

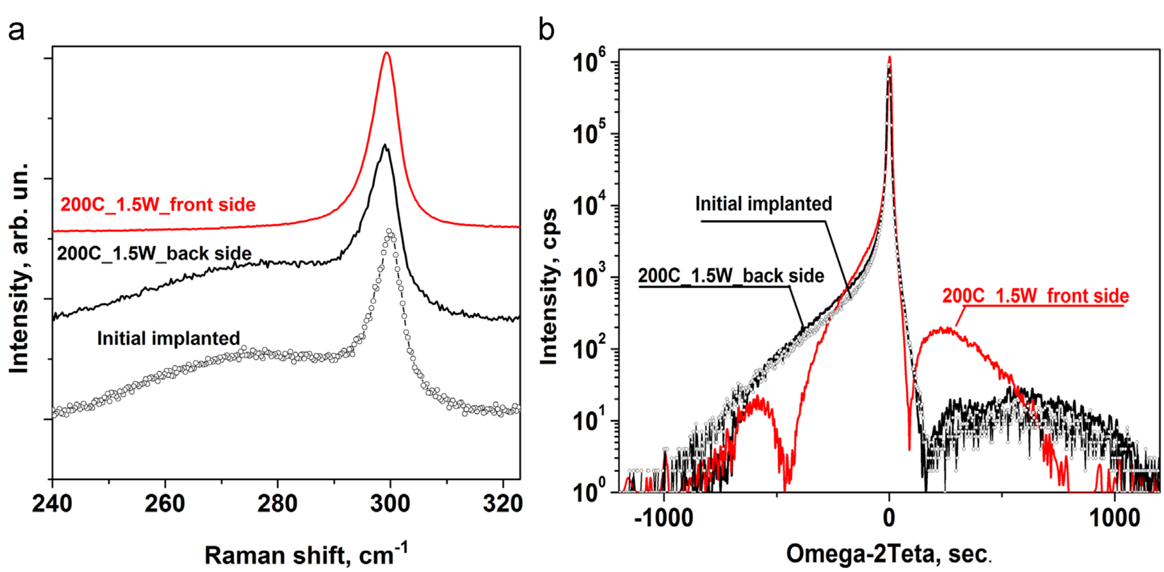

Fig. 4. Raman scattering spectra (a) and $\omega-2\theta$ diffractograms (b) for BF_2^+ -implanted n-Ge after RF plasma treatment ($T=200$ °C, $P=1.50$ W/cm^2, $t=10$ min) of front side and back side of the samples.

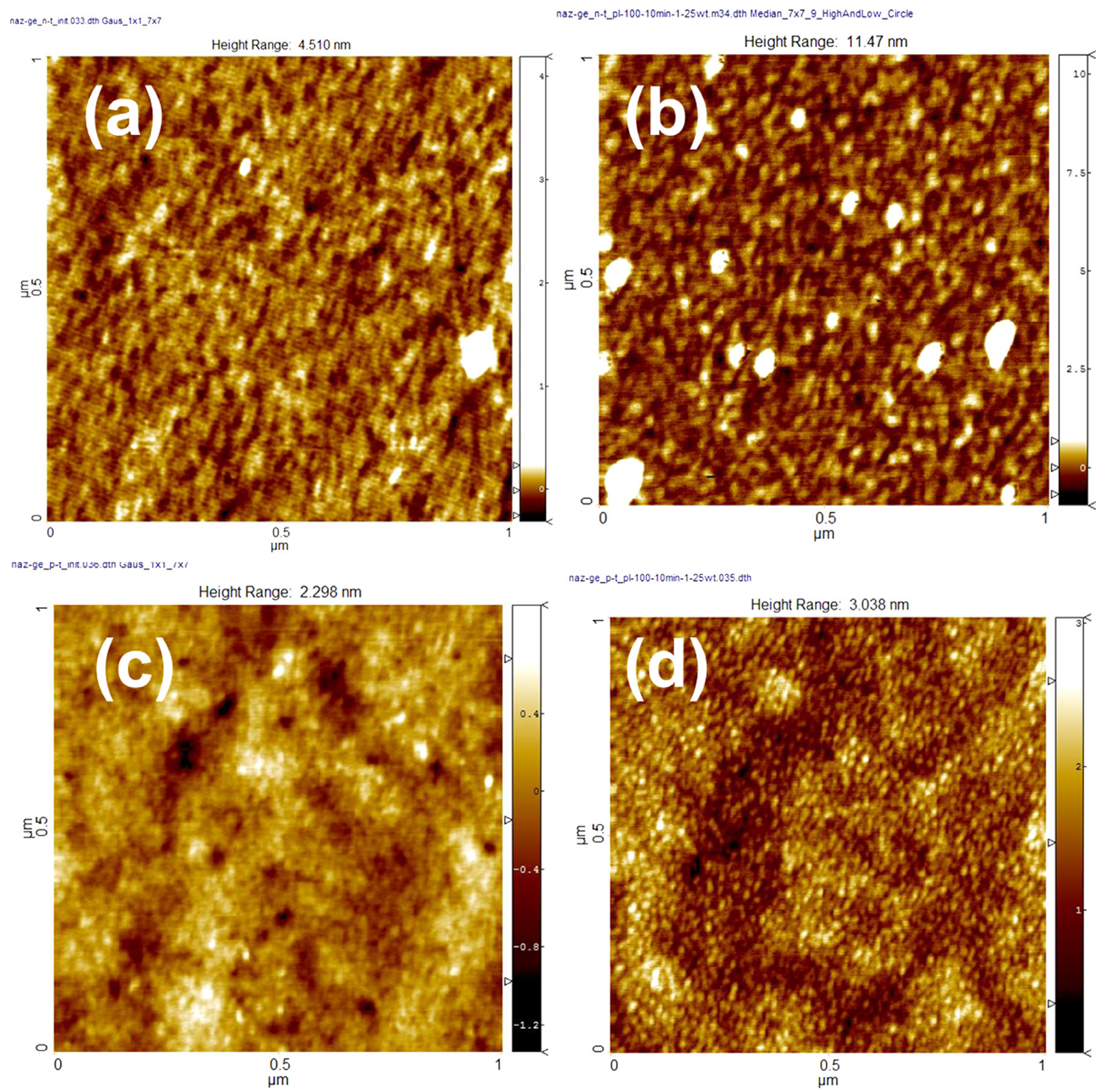

Fig. 5. AFM surface maps of the implanted samples. $BF_2{}^+$-implanted n-Ge: as-implanted (a) and treated by RF plasma (T=100 °C and P=1.25 W/cm^2) (b). P^+- implanted p-Ge: as-implanted (c) and treated by RF plasma treatment (T=100 °C and P=1.25 W/cm^2) (d).

the main factors that influence the implanted layer are the temperature, soft X-ray irradiation and alternating electric field.

The low-energy electron and ion bombardment usually results in slight destruction of thin surface layer that can be shown from AFM experiments (Fig. 5). While the root mean square (RMS) surface roughness of the initial samples of BF_2^+-implanted n-Ge equals to 74.2 pm (Fig. 5(a)), the RMS surface roughness of RF plasma treated samples (T=100 °C and P=1.25 W/cm^2) equals to 229 pm (Fig. 5(b)). Similarly, the RMS surface roughness of P^+-implanted p-Ge is 226 pm (Fig. 5(c)) and increases to 361 pm (Fig. 5(d)) after RF plasma treatment (T=100 °C and P=1.25 W/cm^2). In the latter case we observed the nanostructured surface composed of knolls with the sizes from 20 to 8 nm. Thus the surface destruction is sufficiently low to affect on the ordering and crystallization. So the main factor which can enhance the ordering and crystallization of our amorphous layers is the joint action UV irradiation with the combination of alternating electric field and protons as catalyst of the defect transformation [18].

4. Conclusions

Treatment high-dose implanted shallow Ge layers by the RF plasma in forming gas to results in their crystallization at the temperatures considerably lower than in the case of rapid thermal annealing. This treatment allows to transform the implanted amorphous Ge layer into a thin crystalline layer with sharp interface with the underlying wafer. The observed effects are caused by the nonthermal processes that affect the material during RF plasma treatment, including UV and soft X-ray radiation together with alternating electric field and protons.

Acknowledgments

This work was supported in part by the Science Foundation of Ireland under Grant 09/SIRG/I1623 and in part by the Irish Higher Education Authority Programme for Research in Third-Level Institutions.

References

[1] C. Claeys, E. Simoen, Germanium-Based Technologies: From Materials to Device, Elsevier, Amsterdam, 2007.

[2] R. Duffy, M. Shayesteh, in: Proceedings of the International Workshop on Junction Technology (IWJT), 2014, pp. 155–160.

[3] B.L. Darby, B.R. Yates, N.G. Rudawski, K.S. Jones, A. Kontos, Nucl. Instr. Meth. Phys. Res. B 269 (2011) 20–22.

[4] Y.J. Lee, S.S. Chuang, F.K. Hsueh, H.M. Lin, S.C. Wu, C.Y. Wu, T.Y. Tseng, IEEE Electron Device Lett. 32 (2011) 194–196.

[5] L.P. Chen, T.C. Chou, Appl. Phys. Lett. 68 (1996) 232–234.

[6] C. Wündisch, M. Posselt, B. Schmidt, V. Heera, T. Schumann, A. Mücklich, R. Grötzschel, W. Skorupa, T. Clarysse, E. Simoen, H. Hortenbach, Appl. Phys. Lett. 95 (2009) 252107.

[7] J. Huang, N. Wu, Q. Zhang, C. Zhu, A.A.O. Tay, G. Chen, M. Hong, Appl. Phys. Lett. 87 (2005) 173507.

[8] A.N. Nazarov, V.S. Lysenko, T.M. Nazarova, Semicond. Phys. Quantum Electron. Optoelectron. 11 (2008) 101–123.

[9] V.V. Artamonov, V.S. Lysenko, A.N. Nazarov, B.D. Nechiporuk, V.V. Strelchuk, M.Y.A. Valakh, Physica Status Solidi A 120 (1990) 475–484.

[10] V.S. Lysenko, A.N. Nazarov, S.A. Valiev, I.M. Zaritskii, T.E. Rudenko, A.S. Tkachenko, Physica Status Solidi A 113 (1989) 653–665.

[11] A.N. Nazarov, V.I. Kilchytska, I.P. Barchuk, A.S. Tkachenko, S. Ashok, J. Vac. Sci. Technol. B18 (2000) 1254–1261.

[12] H. Richter, Z.P. Wang, L. Ley, Solid State Commun. 39 (1981) 625–629.

[13] A. Perez-Rodrıguez, A. Romano-Rodrıguez, R. Cabezas, J.R. Morante, T. Jawhari, C.E. Hunt, J. Appl. Phys. 80 (1996) 5736–5741.

[14] C. Moulet, M.S. Goorsky, in: M. Goorsky, (Ed.), Lattice Straine Measurements in Hydrogen Implanted Materials for Layer Transfer Processes, Ion Implantation, InTech, 2012, pp. 65–88 (Open Access Book).

[15] W.-S. Jung, J.-H. Park, A. Nainani, D. Nam, K.C. Saraswat, Appl. Phys. Lett. 101 (2012) 072104.

[16] J.M. Jacques, K.S. Jones, L.S. Robertson, A. Li-Fatou, C.M. Hazelton, E. Napolitani, L.M. Rubin, J. Appl. Phys. 98 (2005) 073521.

[17] M. Ya Valakh, V.S. Lysenko, A.N. Nazarov, G.Yu Rudko, A.S. Tkachenko, N.I. Shakhraychuk, Nucl. Instrum. Methods Phys. Res. B44 (1989) 146–148.

[18] A.N. Nazarov, V.M. Pinchuk, T.V. Yanchuk, V.S. Lysenko, Ya. N. Vovk, S. Rangan, S. Ashok, V. Kudoyarova, E.I. Terukov, Int. J. Hydrogen Energy 26 (2001) 521–526.tp